NASA Technical Paper 1236

Evaluation of a Hybrid, Anisotropic, Multilayered, Quadrilateral Finite Element

James C. Robinson and Charles L. Blackburn

AUGUST 1978

NASA

*MSG DI4 DROLS PROCESSING - LAST INPUT IGNORED

-- 1 OF 1
-- ***DTIC DOES NOT HAVE THIS ITEM***
-- 1 - AD NUMBER: D425647
-- 5 - CORPORATE AUTHOR: NATIONAL AERONAUTICS AND SPACE ADMINISTRATION
-- HAMPTON VA LANGLEY RESEARCH CENTER
-- 6 - UNCLASSIFIED TITLE: EVALUATION OF A HYBRID, ANISOTROPIC,
-- MULTILAYERED, QUADRILATERAL FINITE ELEMENT,
--10 - PERSONAL AUTHORS: ROBINSON ,J. C. ;BLACKBURN,C. L. ;
--11 - REPORT DATE: AUG , 1978
--12 - PAGINATION: 28P
--14 - REPORT NUMBER: NASA TP-1236, L-12113
--20 - REPORT CLASSIFICATION: UNCLASSIFIED
--22 - LIMITATIONS (ALPHA): APPROVED FOR PUBLIC RELEASE; DISTRIBUTION
-- UNLIMITED. AVAILABILITY: NATIONAL TECHNICAL INFORMATION SERVICE,
-- SPRINGFIELD, VA. 22161. NASA TP 1236.
--33 - LIMITATION CODES: 1
--******
-- END OF DISPLAY LIST

-- ((ENTER NEXT COMMAND))

NASA Technical Paper 1236

Evaluation of a Hybrid, Anisotropic, Multilayered, Quadrilateral Finite Element

James C. Robinson
Langley Research Center
Hampton, Virginia

and

Charles L. Blackburn
University of Tennessee at Nashville
Nashville, Tennessee

National Aeronautics
and Space Administration

**Scientific and Technical
Information Office**

1978

SUMMARY

A hybrid, anisotropic, multilayered, quadrilateral finite element with bending-extensional coupling is evaluated. Analyses performed in the evaluation include the following: (1) Buckling of general laminated plates; (2) thermal stresses of laminated plates cured at elevated temperatures; (3) displacements of a bimetallic beam; and (4) displacement and stresses of a single-cell box beam with warped cover panels. Also, displacements and stresses for flat and spherical orthotropic and anisotropic segments are compared with results from higher order plate and shell finite-element analyses. The calculations demonstrate the usefulness of this element for the analysis of practical composite structures.

INTRODUCTION

Finite-element analysis of structures composed of fiber-reinforced advanced-composite materials involves complications not encountered in the analysis of structures of isotropic materials. The highly orthotropic stiffness, strength, and thermal properties of the individual layers require that either the orientation and properties of each layer be defined or the equivalent anisotropic properties of the laminate be specified.

The low stiffness and strength normal to the fiber direction of a single layer require that several layer orientations be used in practical structures. In some cases, it may not be possible or practical to use laminates that are symmetric about their midplane. For such laminates, bending-extensional coupling exists and must be considered in the analysis if an accurate estimate of laminate behavior is to be obtained (refs. 1 and 2).

When simple two-dimensional structural finite elements (i.e., having three or four nodes) are used, quadrilateral elements are preferable to triangular elements because they yield more accurate results for a given number of degrees of freedom (refs. 3 and 4). Generally, for curved structures it is impossible to guarantee that all four nodes of a quadrilateral are in a plane. Therefore, the availability of a simple quadrilateral finite element capable of accommodating small amounts of warping (i.e., not all four nodes in a plane) is desirable for general purpose applications. Previously used approximate methods, which allow for small amounts of warping of simple quadrilateral elements, have been described in references 3 to 7.

The development of a hybrid, anisotropic, quadrilateral element, which accounts for bending-extensional coupling and recovery of layer stresses, is described in reference 8 and briefly summarized herein. This element was incorporated, under NASA contract, in the SPAR structural analysis system (refs. 9 and 10). As part of the validation of this new element, the following studies have been conducted:

(1) Buckling of general laminated plates

(2) Thermal stresses of laminated plates cured at elevated temperatures

(3) Displacements of a bimetallic beam

(4) Displacements and stresses of warped isotropic and anisotropic panels

Flat and spherical orthotropic and anisotropic segments are also analyzed, and the results are compared with results from higher order plate and shell finite-element analyses.

The purpose of this paper is to document results obtained with the new element in a variety of applications to establish its accuracy and usefulness.

SYMBOLS

Values are given in both SI and U.S. Customary Units. The calculations and measurements were made in U.S. Customary Units.

a,b	plate dimensions parallel to X- and Y-axes, respectively
$\mathcal{R}$	aspect ratio, a/b
$\bar{D}_{11}$	flexural stiffness of unidirectional laminate
E_T	elastic modulus normal to fibers
f	rise of shallow shell (fig. 9)
F	force
h	semidepth of box beam (fig. 6)
Δh	out of planeness (fig. 6)
M_X	bending-moment resultant
N	normal-stress resultant
N_{XY}	shearing-stress resultant
p	intensity of uniform pressure loading
R	radius of curvature of spherical shell
t	thickness of shell
u,v,w	displacements parallel to X-, Y-, and Z-axes, respectively
w_f	normal displacement of flat panel at node 6 (fig. 4)

x,y,z	Cartesian coordinates
X,Y,Z X_1,Y_1,Z_1 X_2,Y_2,Z_2 $\bar{X},\bar{Y},\bar{Z}$	Cartesian axes system
α,β	angles of rotation for warping transformation (fig. 1)
ϵ	normal strain
θ	fiber orientation or rotational displacement
κ	curvatures
σ	normal stress
$\bar{\sigma}$	von Mises effective stress
τ_{XY}	shear stress in X-Y plane

Subscripts:

f	flat panel
X,Y,Z $\bar{X},\bar{Y}$	direction of component
$1,2,3,4$	node number

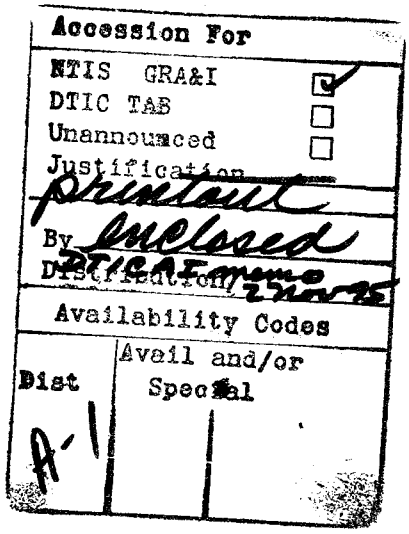

DESCRIPTION OF THE ELEMENT

Flat membrane and bending quadrilateral elements were developed by Pian, based on the method of minimum complementary energy (ref. 11). In this method an element stress distribution, which identically satisfies the equilibrium conditions for generalized plane stress when transverse shear deformation is neglected, is assumed. Inplane translations and out-of-plane rotations are assumed to vary linearly along the edges of the membrane and bending elements, respectively. The normal displacement is assumed to have a cubic variation along the edges of the bending element.

The flat quadrilateral element of reference 11 was modified in reference 8 to provide structural analysis capability for practical composite structures. These modifications include the following:

(1) Use of the orthotropic properties of each layer to permit modeling of laminated structures and the recovery of layer stresses

(2) Inclusion of bending-extensional coupling associated with unsymmetrical laminates

(3) An approximate formulation to account for a small amount of element warping; that is, not all four nodes in a plane

Laminate Properties

Orthotropic material properties of the layer are specified by a 3×3 matrix [A] relating the stress resultants and the inplane strains and another 3×3 matrix [D] relating the moment resultants and the plate curvatures

$$\begin{Bmatrix} N \\ M \end{Bmatrix} = \begin{bmatrix} A & B \\ B^T & D \end{bmatrix} \begin{Bmatrix} \epsilon \\ \kappa \end{Bmatrix} \tag{1}$$

Provision for bending-extensional coupling is provided by generating the 3×3 coupling matrix [B], which relates extensional and bending terms.

Warping

A quadrilateral element is defined by the specification of the bounding nodes in a particular order. Element properties are referred to a coordinate system based on these nodal locations; for a flat element, this is usually the plane of the element. If all four nodes are not coplanar, the element is referred to herein as being warped. For such an element, several possible reference planes can be defined, and the one used here is that defined by the first three nodes. Warping is defined as the ratio of the distance from the fourth node to the reference plane and the square root of the area.

The method used to approximate the change in the intrinsic stiffness matrix due to warping is based on a transformation applied to the intrinsic deformation vector of node 4. Intrinsic refers to the properties of an element that is statically determinately supported; that is, without rigid-body contributions. The transformation assumes that node 4 has planar stiffness that is directed through node 2. Figure 1 shows the steps used in the development of the transformation vector. A more detailed discussion is in the appendix.

RESULTS AND DISCUSSION

This section presents several problem solutions obtained with the new element and compares them with existing solutions. The problems include (1) the buckling loads for laminated anisotropic plates; (2) thermal curing

stresses in laminated panels; (3) displacements of a bimetallic beam; (4) displacement and stresses of a box beam with warped isotropic cover panels; (5) deflection of a box beam with warped anisotropic cover panels; and (6) displacements and stress resultants for flat and spherical orthotropic and anisotropic segments.

Buckling of Laminated Anisotropic Panels

The ability to predict buckling loads of flat, multilayered, anisotropic panels with this element is demonstrated by comparison with results from an extended Galerkin analysis (ref. 12). Nondimensional shear and axial buckling loads from reference 12 and for several finite-element mesh sizes are shown in tables 1 and 2 for square and long, thin rectangular panels. The positive sign conventions are defined by the sketches shown in each table. As indicated by these results, convergence of the finite-element solution has been attained for all practical purposes. Furthermore, these results correlate well with the Galerkin solution except in two cases for two-layer panels with a 45^{o} fiber orientation. A 25-percent difference occurred for the shear buckling load of a square panel (table 1) and a 19-percent difference occurred in the axial buckling load of a rectangular panel (table 2). Both differences may be attributed to nonconvergence of the Galerkin solution, which gave higher buckling loads than the monotonically decreasing converged finite-element solutions.

Thermal Curing Stresses in Laminated Panels

Thermal stresses due to the high temperature curing of multilayered, graphite-epoxy panels have been calculated to demonstrate the capability of the new element to recover layer stresses. Two, three-layered laminates, namely, [15/-15/15] and $[0/90_{10}/0]$ (i.e., a middle layer 10 times thicker than either outer layer) are analyzed (fig. 2). The stresses within each layer are compared with the results from a closed-form solution in reference 13 (corrected by the authors) for an identical panel. As table 3 indicates, nearly identical results are obtained. The results for the angle ply [15/-15/15] laminate were corrected to eliminate an error in reference 13 because of the difference between engineering and tensor components of the thermal strains (a factor of 2).

Deflection of a Bimetallic Strip

In order to evaluate the bending-extensional coupling capability of the elements, deflections were calculated for the laminated steel-aluminum plate strip subjected to three different loads (fig. 3); namely, unit axial load, moment, and transverse force. Deflections are compared with those from a closed-form solution which assumes cylindrical bending (ref. 14). A comparison of displacements is presented in table 4 and shows a difference of less than 0.1 percent.

Analysis of a Box Beam With Warped Isotropic Cover Panels

An assessment of the effect of warping on the new element and two other quadrilateral elements from reference 15 is shown in figure 4. The other elements, QMC and QMB5, are based on an assumed displacement field and an assumed stress field (ref. 15). Neither of the latter elements contains any correction for warping. In the structure shown, node 7 is above the plane of nodes 5, 6, and 8 and $h/a = 0.05$, except as noted. Only one-half of the symmetric box beam is shown, and it is composed of a membrane element for the cover panel supported by shear webs along the sides and rod elements at the corners.

Since the element representing the cover panel is warped, four different reference planes can be obtained, depending on the order of numbering the nodes. Results using different reference planes are different; consequently the warping correction is dependent on the node numbering sequence. The largest difference between the four possible results is defined as the scatter. The present element produces a scatter in the normal displacement at node 6 of approximately 7 percent for $\Delta h/a = 0.04$. This scatter is significantly less than the 130-percent scatter for the QMC and QMBS elements. When calculations were repeated for $h/a = 0.10$, the scatter for the new element is approximately 5 percent. Figure 5 indicates a scatter in the von Mises stress due to warping of the isotropic membrane element of less than 4 percent for $h/a = 0.10$ and approximately 6 percent for $h/a = 0.05$.

Analysis of a Box Beam With Warped Anisotropic Cover Panels

A similar study for laminated composites was conducted. Warping is incorporated only in the membrane stiffnesses. The new laminated element includes bending and extensional stiffness. For a single, very thin, warped quadrilateral (as in the box beam in fig. 6) there are noticeable differences between the behavior of an element having only membrane stiffness and one having both membrane and bending stiffness. These differences are caused by the different assumptions used in expanding the intrinsic stiffness matrix to the full stiffness matrix in the membrane and bending elements, as discussed in the appendix. Because of these differences and the fact that SPAR prohibits the specification of laminated properties for membrane elements (because of the possibility of bending-extensional coupling), it was necessary to calculate the A-matrix (eq. (1)) of the complete laminate and to input this as the membrane properties for a single layer. Results are shown in figure 6, and for a quasi-isotropic ($[90/0/\pm45]_S$) laminate are similar to the isotropic results, as would be expected. However, a scatter of nearly 40 percent is obtained for an orthotropic ($[90/0/90/0]_S$) laminate.

The present treatment of warping is an improvement over the previously studied elements, which are not corrected for warping. However, care must be exercised in the use of the new element for warped structures to insure that satisfactory results are obtained.

Comparison With Higher Order Elements

Description of higher order elements.- Results obtained with the new element are compared with results obtained by using several higher order quadrilateral elements for some plate and shell problems analyzed in reference 16. The higher order elements are based on linear shallow-shell theory, including effects of shear deformation, material anisotropy, and bending-extensional coupling. Two elements, designated SQ12 and SQH, are based on assumed displacement fields. The SQ12 element has 12 nodes and 60 (shell) or 36 (plate) degrees of freedom, and the SQH element has four nodes and 80 (shell) or 48 (plate) degrees of freedom. A third element, designated MQ8, is an eight-node quadrilateral, mixed formulation element having 104 (shell) and 64 (plate) degrees of freedom.

Plate.- Displacement and moment distributions were calculated for uniformly loaded, clamped, orthotropic [0/90/0/90/0/90/0/90/0] and uniformly loaded, simply supported, anisotropic [45/-45/45/-45/45/-45/45/-45/45] square plates, having thickness-to-side ratios t/a of 0.01 and 0.001. Since the new element does not include the effects of transverse shear deformations, example problems in which the effect of shear deformation is very small were selected. Results were obtained by using 4×4 and 8×8 finite-element meshes (for the complete model) and are compared with results from reference 16 in figures 7 and 8. Results for the 8×8 mesh are nearly coincident with results for the higher order elements for both plates. Results for the 4×4 finite-element mesh are also in good agreement with reference 16.

Shallow shell.- The present element is compared with displacements and load distributions for uniformly loaded, shallow, spherical shell segments (fig. 9). These shell segments are simply supported, nine-layered, orthotropic and anisotropic laminates, and all elements of the models are warped. Again, results were obtained by using 4×4 and 8×8 finite-element meshes. Comparisons are given in figures 10 and 11. In general, results using the 8×8 mesh are in excellent agreement with reference 16. The exceptions occurred for the peak and near-peak bending moment of the orthotropic spherical shell with $t/a = 0.001$ (fig. 10(f)).

Results obtained with the 4×4 mesh were generally in good agreement with reference 16 but displayed some error near the crown of the shell ($x/a = 0.5$). Also, the shell results for the 4×4 mesh are less accurate than the plate results.

Finally, note that, compared with the higher order elements of reference 16, more new elements are needed to obtain the same level of accuracy. However, use of the higher order elements, which have strains as nodal degrees of freedom or multiple nodes per side, is not strictly applicable to some practical structural situations, such as abrupt thickness or stiffness changes or multiple stiffeners. Conversely, the new element has no such restrictions.

CONCLUSIONS

An evaluation of a hybrid, anisotropic, quadrilateral element with bending-extensional coupling and capability to recover inplane, layer stresses has been performed. The following studies have been conducted in this evaluation:

(1) Buckling of general laminated plates

(2) Thermal stresses of laminated plates cured at elevated temperatures

(3) Displacements of a bimetallic beam

(4) Displacements and stresses in warped isotropic and anisotropic panels

(5) Displacements and stresses for flat and spherical orthotropic and anisotropic segments

For the new element, the following conclusions can be made:

1. Accurate results can be obtained for the buckling characteristics of flat laminated plates.

2. Thermal curing stresses can be accurately determined.

3. The accuracy of the bending-extensional coupling capability is substantiated by the excellent correlation with exact results for a bimetallic strip.

4. The dependence of the results on the order of numbering the element nodes for a warped panel is reduced but is still significant; thus, care must be exercised in the use of this element for panels which are not flat.

5. The new element displays generally good agreement with results from several higher order elements for orthotropic and anisotropic plate and shell configurations.

This evaluation indicates that this element has broad application to the analysis of practical structures.

Langley Research Center
National Aeronautics and Space Administration
Hampton, VA 23665
May 10, 1978

APPENDIX

TRANSFORMATION FOR WARPING

The reference frame for node 4 is shown in figure 1(a) and is nearly parallel to the element reference frame when the warping is small. The transformation from the element reference frame to the node 4 reference frame is shown in figures 1(b) to 1(d) and is defined by the following sequence:

(1) From a coordinate system, at node 4, that is parallel to the element reference frame, rotate through an angle $90^\circ - \alpha$ (fig. 1(b)) about the Z-axis so that node 2 lies in the Y_1-Z_1 plane. The transformation describing this rotation is

$$\{X_1\} = [T_1]\{X\} \tag{A1}$$

where T_1 is the coordinate transformation matrix

$$\begin{bmatrix} \cos(90^\circ - \alpha) & \sin(90^\circ - \alpha) & 0 \\ -\sin(90^\circ - \alpha) & \cos(90^\circ - \alpha) & 0 \\ 0 & 0 & 1 \end{bmatrix} \tag{A2}$$

(2) Rotate through an angle β (fig. 1(c)) about the X_1-axis so that the Y_2-axis passes through node 2; thus,

$$\{X_2\} = [T_2]\{X_1\} \tag{A3}$$

(3) Rotate through an angle $\alpha - 90^\circ$ (fig. 1(d)) about the Z_2-axis to the assumed original reference frame for node 4; thus,

$$\{\bar{X}\} = [T_3]\{X_2\} \tag{A4}$$

and the complete transformation from the element reference frame to the node 4 reference frame is

$$\{\bar{X}\} = [T_3][T_2][T_1]\{X\} = [T]\{X\} \tag{A5}$$

The transformation of the forces at node 4 uses the same matrix; thus,

$$\begin{Bmatrix} F_{\bar{X},4} \\ F_{\bar{Y},4} \\ 0 \end{Bmatrix} = [T] \begin{Bmatrix} F_{X,4} \\ F_{Y,4} \\ F_{Z,4} \end{Bmatrix} \tag{A6}$$

or

$$\begin{Bmatrix} F_{X,4} \\ F_{Y,4} \\ F_{Z,4} \end{Bmatrix} = [T]^T \begin{Bmatrix} F_{\bar{X},4} \\ F_{\bar{Y},4} \\ 0 \end{Bmatrix} \tag{A7}$$

The intrinsic stiffness matrix k (ref. 8) for a flat quadrilateral has five degrees of freedom and is expressed by

$$\begin{Bmatrix} F_{X,2} \\ F_{X,3} \\ F_{Y,3} \\ F_{X,4} \\ F_{Y,4} \end{Bmatrix} = [k_f] \begin{Bmatrix} u_{X,2} \\ u_{X,3} \\ u_{Y,3} \\ u_{X,4} \\ u_{Y,4} \end{Bmatrix} \tag{A8}$$

where the forces and displacements are defined in figure 12.

The transformation of the matrix in equation (A8) to include warping effects is now derived using the nodal force transformation

$$\begin{Bmatrix} F_{X,2} \\ F_{X,3} \\ F_{Y,3} \\ F_{X,4} \\ F_{Y,4} \\ F_{Z,4} \end{Bmatrix} = [C]^T \begin{Bmatrix} F_{X,2} \\ F_{X,3} \\ F_{Y,3} \\ F_{\bar{X},4} \\ F_{\bar{Y},4} \\ 0 \end{Bmatrix} \tag{A9}$$

where

$$[C]^T = \left[\begin{array}{c|c} I & 0 \\ \hline 0 & T^T \end{array}\right]$$

The Z-force at node 4, $F_{Z,4}$, has been introduced by the coordinate transformation. The intrinsic stiffness matrix for the warped element is obtained by

$$[k_w] = [C]^T[k_f][C] \tag{A10}$$

Equation (A10) results in a modified 6 × 6 intrinsic stiffness matrix, which accounts for warping.

Before the element stiffness matrices can be combined, the 6 × 6 intrinsic matrices must be expanded to include all degrees of freedom in the element (for the present element the result is a 12 × 12 matrix). The expansion, a standard procedure whenever the intrinsic representation is used, is accomplished by a transformation similar to equation (A10) in which a 6 × 12 transformation matrix is used. The 6 × 12 matrix is determined (by statics) from the relationship between the intrinsic forces and the total set of nodal forces (fig. 12). The numerical evaluation of the matrix is straightforward, but a general algebraic representation of the terms is lengthy and, thus, has not been included here.

For elements having bending, as well as membrane stiffness, the out-of-plane force balance is not statically determinate, and an assumption is required as to the distribution of the out-of-plane forces. In this case, it is assumed that the out-of-plane force due to warping at node 4 is reacted by an out-of-plane force at node 1. This assumption should be satisfactory for problems where the out-of-plane stiffness due to bending predominates or where several elements contribute to the out-of-plane stiffness of the joint.

REFERENCES

1. Ashton, J. E.; Halpin, J. C.; and Petit, P. H.: Primer on Composite Materials: Analysis. Technomic Pub. Co., Inc., c.1969.

2. Jones, Robert M.: Mechanics of Composite Materials. McGraw-Hill Book Co., c.1975.

3. Turner, M. J.; Clough, R. W.; Martin, H. C.; and Topp, L. J.: Stiffness and Deflection Analysis of Complex Structures. J. Aeronaut. Sci., vol 23, no. 9, Sept. 1956, pp. 805-823, 854.

4. Robinson, John: A Warped Quadrilateral Strain Membrane Element. Comput. Methods Appl. Mech. & Eng., vol. 7, no. 3, 1976, pp. 359-367.

5. Argyris, J. H.; and Kelsey, S.: Modern Fuselage Analysis and the Elastic Aircraft - Basic Theory. Butterworths, 1963.

6. Taig, I. C.; and Kerr, R. I.: Some Problems in the Discrete Element Representation of Aircraft Structures. Matrix Methods of Structural Analysis, B. Fraeijs de Veubeke, ed., AGARDograph 72, Macmillan Co., 1964, pp. 267-315.

7. MacNeal, Richard H., ed.: The NASTRAN Theoretical Manual. NASA SP-221, 1970.

8. Whetstone, W. D.; Yen, C. L.; and Jones, C. E.: SPAR Structural Analysis System Reference Manual - System Level 11. Volume 2 - Theory. NASA CR-145098-2, 1977.

9. Whetstone, W. D.: SPAR Structural Analysis System Reference Manual - System Level 11. Volume 1 - Program Execution. NASA CR-145098-1, 1977.

10. Giles, Gary L.; and Haftka, Raphael T.: SPAR Data Handling Utilities. NASA TM-78701, 1978.

11. Pian, Theodore H. H.: Derivation of Element Stiffness Matrices by Assumed Stress Distributions. AIAA J., vol. 2, no. 7, July 1964, pp. 1333-1336.

12. Sawyer, James Wayne: Flutter and Buckling of General Laminated Plates. J. Aircr., vol. 14, no. 4, Apr. 1977, pp. 387-393.

13. Tsai, Stephen W.: Strength Characteristics of Composite Materials. NASA CR-224, 1965.

14. Calcote, Lee R.: The Analysis of Laminated Composite Structures. Van Nostrand Reinhold Co., c.1969.

15. Haftka, Raphael T.; and Robinson, James C.: Effect of Out-of-Planeness of Membrane Quadrilateral Finite Elements. AIAA J., vol. 11, no. 5, May 1973, pp. 742-744.

16. Noor, Ahmed K.; and Mathers, Michael D.: Shear-Flexible Finite-Element Models of Laminated Composite Plates and Shells. NASA TN D-8044, 1975.

TABLE 1.- COMPARISON OF AXIAL AND SHEAR BUCKLING LOAD FROM EXTENDED GALERKIN SOLUTION (REF. 12) AND VARIOUS FINITE-ELEMENT MESH SIZES FOR SQUARE PANEL

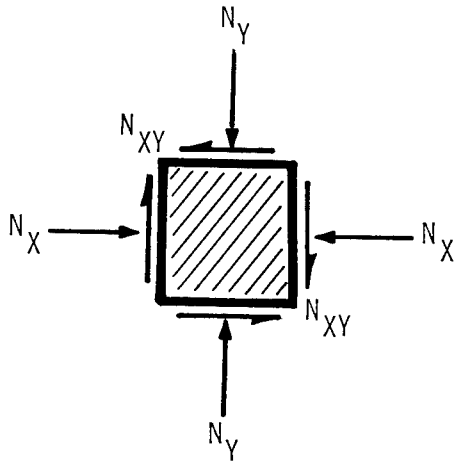

Stacking sequence	Ref. 12	Mesh		
		4 × 4	6 × 6	8 × 8
Axial buckling load = $\frac{N_X b^2}{\bar{D}_{11}\pi^2}$				
[0]	1.306	1.307	1.304	1.303
[90]	.890	.931	.902	.896
$[-45]_s$	1.576	1.583	1.507	1.478
$[45/-45]_s$	1.900	1.913	1.865	1.849
$[-45/45/-45]_s$	2.080	2.112	2.087	2.080
Shear buckling load = $\frac{N_{XY} b^2}{\bar{D}_{11}\pi^2}$				
[0]	2.880	3.069	2.984	2.927
[90]	2.880	3.069	2.984	2.894
$[-45]_s$	7.850	7.929	7.744	7.698
	-2.120	-1.851	-1.637	-1.584
$[45/-45]_s$	7.180	7.355	7.170	7.135
	-2.670	-2.818	-2.601	-2.550
$[-45/45/-45]_s$	6.440	6.660	6.470	6.437
	-3.530	-3.752	-3.539	-3.493

TABLE 2.- COMPARISON OF AXIAL AND SHEAR BUCKLING LOAD FROM EXTENDED GALERKIN SOLUTION (REF. 12) AND VARIOUS FINITE-ELEMENT MESH SIZES FOR RECTANGULAR PANEL; $\mathcal{R}$ = 10

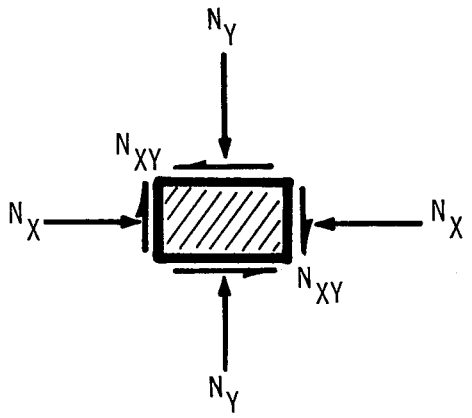

Stacking sequence	Ref. 12	Mesh		
		2 × 10	2 × 20	4 × 20
Axial buckling load = $\frac{N_X b^2}{\bar{D}_{11}\pi^2}$				
[0]	0.869	0.926	0.899	0.870
[90]	.860	1.359	.915	.892
$[-45]_s$	1.560	1.568	1.344	1.272
$[45/-45]_s$	1.850	2.014	1.804	1.754
$[-45/45/-45]_s$	2.070	2.116	2.118	2.076
Shear buckling load = $\frac{N_{XY} b^2}{\bar{D}_{11}\pi^2}$				
[0]	0.914	0.966	1.047	0.798
[90]	2.330	4.680	2.955	2.724
$[-45]_s$	3.890	4.549	4.368	3.894
	-.890	-1.018	-1.041	-.848
$[45/-45]_s$	3.560	4.197	4.004	3.581
	-1.340	-1.616	-1.533	-1.324
$[-45/45/-45]_s$	3.200	3.794	3.602	3.233
	-1.780	-2.151	-2.021	-1.789

TABLE 3.- COMPARISON OF THERMAL CURING STRESSES IN SQUARE, GRAPHITE-EPOXY PANEL AT 405.4 K (270° F) WITH EXACT SOLUTION OF REFERENCE 13

Layer	Present element						Reference 13					
	σ_X		σ_Y		τ_{XY}		σ_X		σ_Y		τ_{XY}	
	MPa	psi	MPa	psi	MPa	psi	MPa	psi	MPa	psi	MPa	psi
$[0/90_{10}/0]$												
1	9.797	1421.0	-4.392	-637.0	0	0	9.791	1420.0	-4.413	-640.0	0	0
2	-48.987	-7105.0	21.960	3185.0	0	0	-48.953	-7100.0	22.063	3200.0	0	0
3	9.797	1421.0	-4.392	-637.0	0	0	9.791	1420.0	-4.413	-640.0	0	0
*[15/-15/15]												
1	1.225	177.6	0.216	31.3	-4.942	-716.8	1.225	177.7	0.216	31.3	-4.942	-716.8
2	-2.449	-355.2	.432	-62.6	9.884	1433.6	-2.450	-355.3	.432	-62.7	9.885	1433.7
3	1.225	177.6	.216	31.3	-4.942	-716.8	1.225	177.7	.216	31.3	-4.942	-716.8

*Corrected reference 13 values.

TABLE 4.- DISPLACEMENTS OF LAMINATED STEEL-ALUMINUM PLATE STRIP DUE TO VARIOUS TYPES OF UNIT LOADS

Load	Present element					Reference 14				
	u		w		θ	u		w		θ
	nm	in.	nm	in.	μrad	nm	in.	nm	in.	μrad
Axial	7.1572	0.28178×10^{-6}	-25.456	-0.10022×10^{-5}	0.20045	7.1577	0.28180×10^{-6}	-25.451	-0.10020×10^{-5}	0.20040
Transverse	-25.4572	-1.00225	715.729	2.81783	-4.22674	-25.4508	-1.00200	715.772	2.81800	-4.22700
Bending	5.0914	.20045	-107.358	-.42267	.84535	5.0902	.20040	-107.366	-.42270	.84540

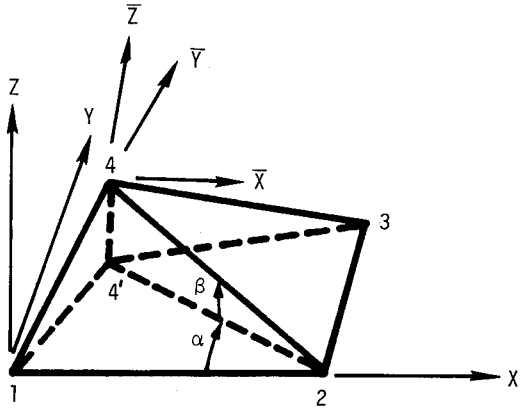

(a) Coordinate systems.

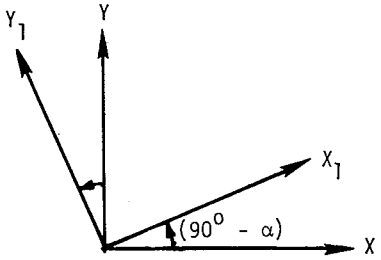

(b) Rotation about Z-axis.

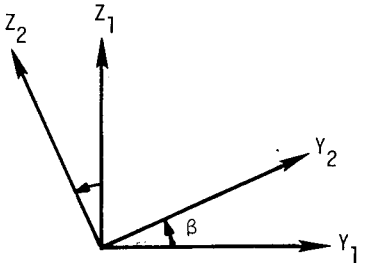

(c) Rotation about X_1-axis.

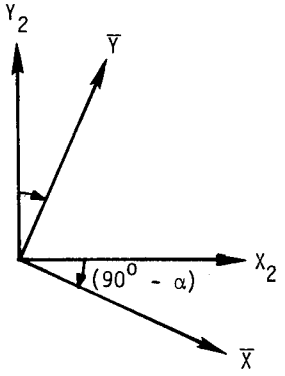

(d) Rotation about Z_2-axis.

Figure 1.- Coordinate transformation for node 4 used to develop warping correction.

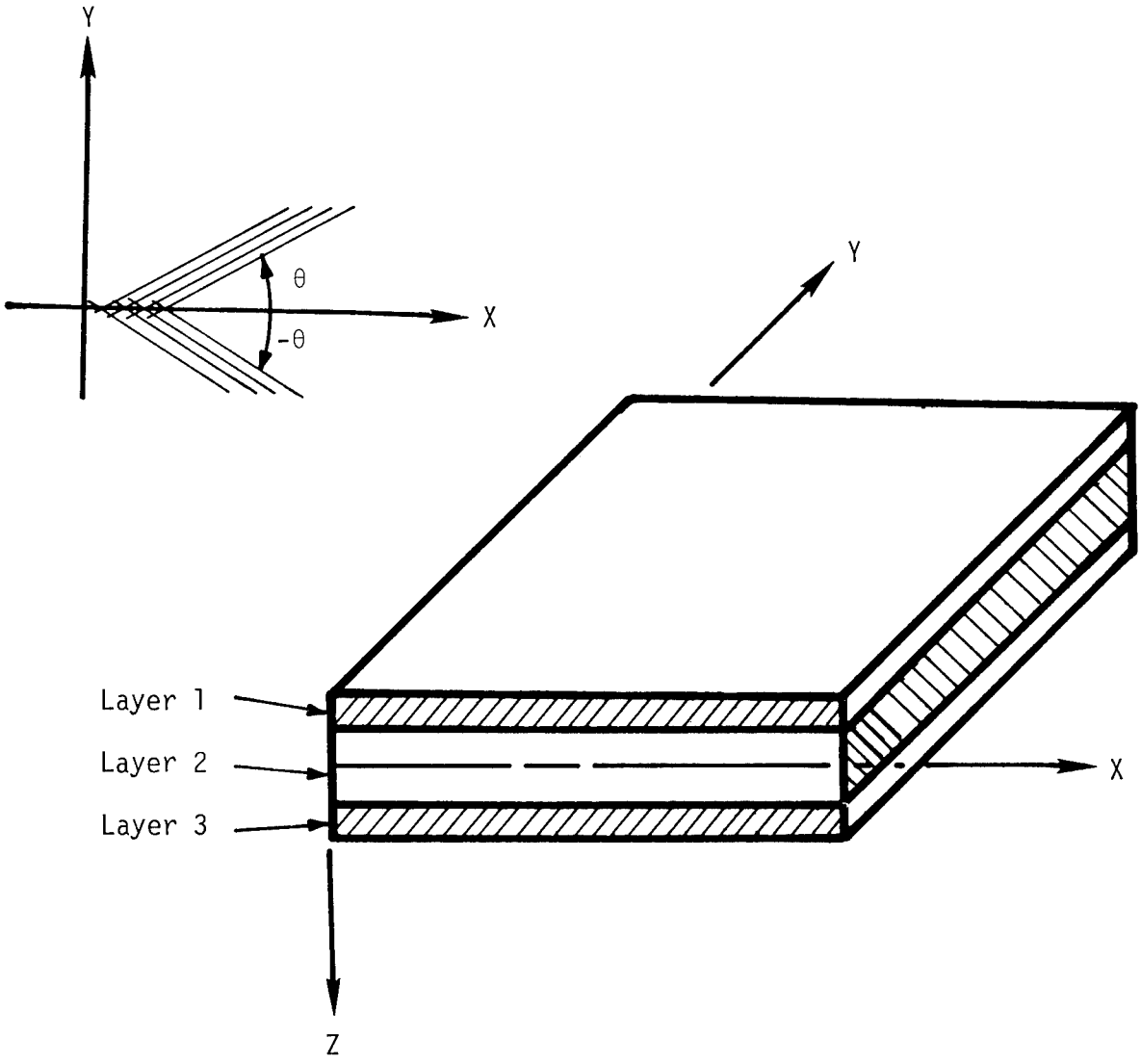

Figure 2.- Schematic diagram showing coordinate system, layer location, and fiber orientation for thermal-stress data interpretation.

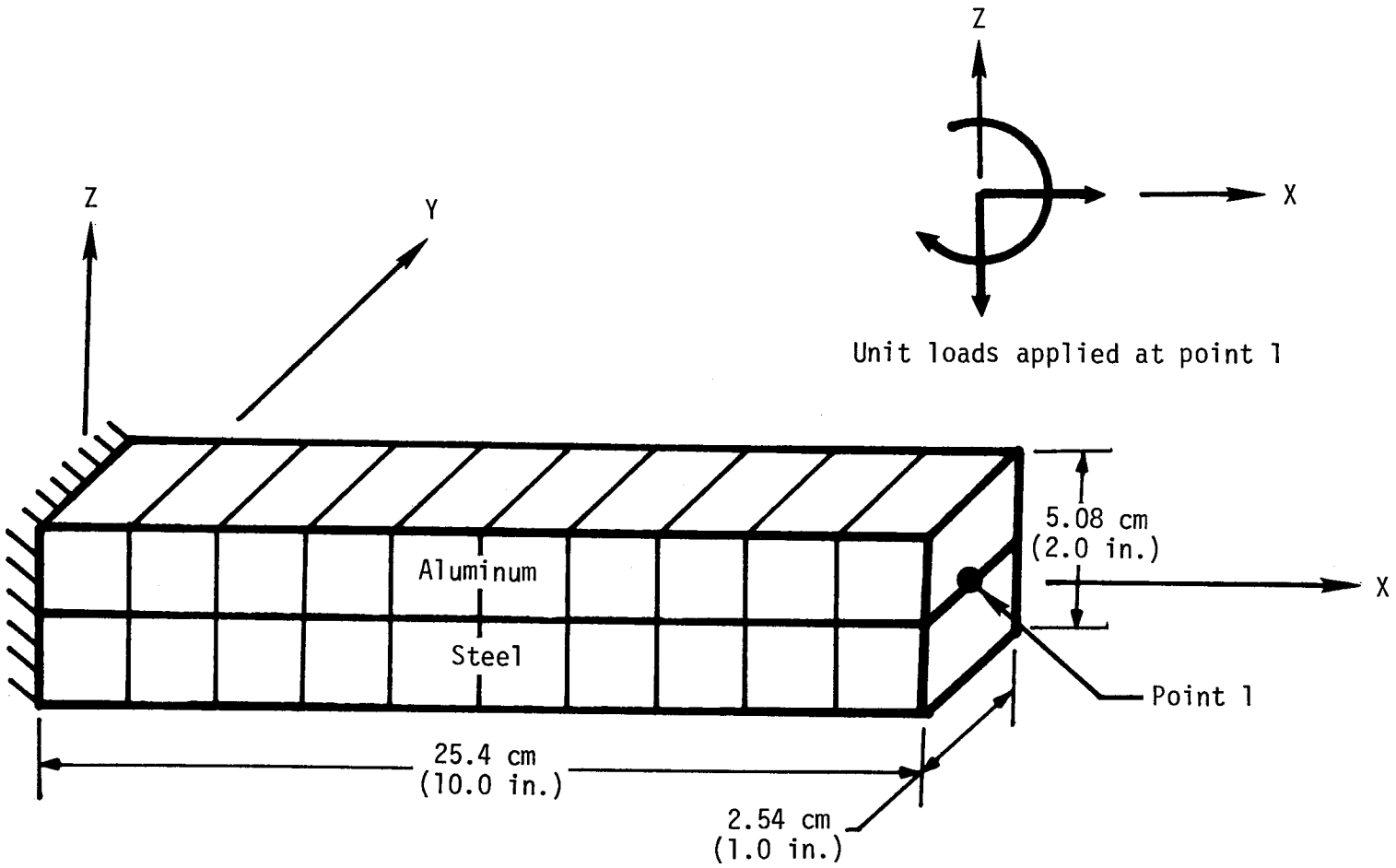

Figure 3.- Finite-element model of laminated steel-aluminum plate strip.

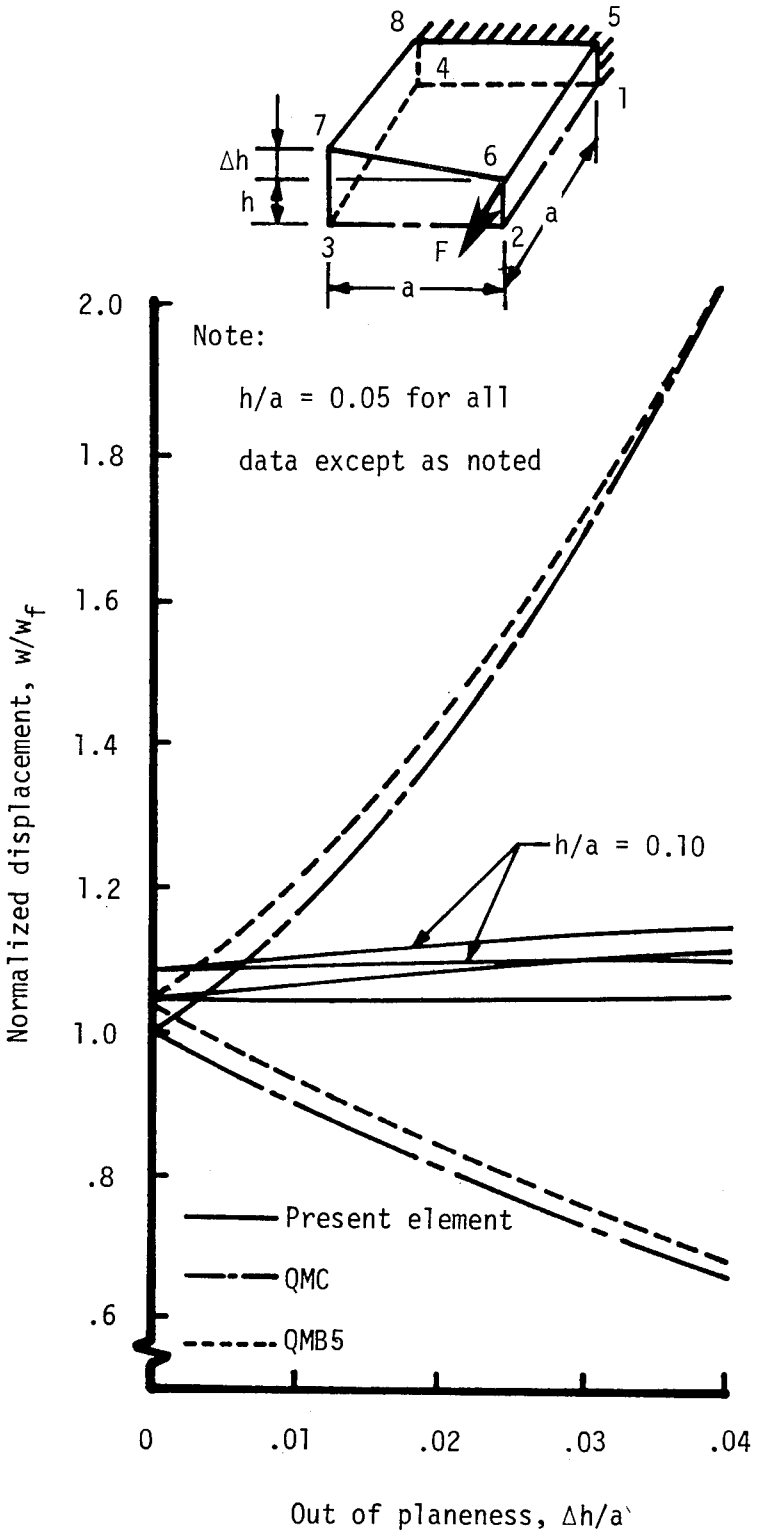

Figure 4.- Scatter of results for normal displacement at node 6 due to out of planeness of node 7.

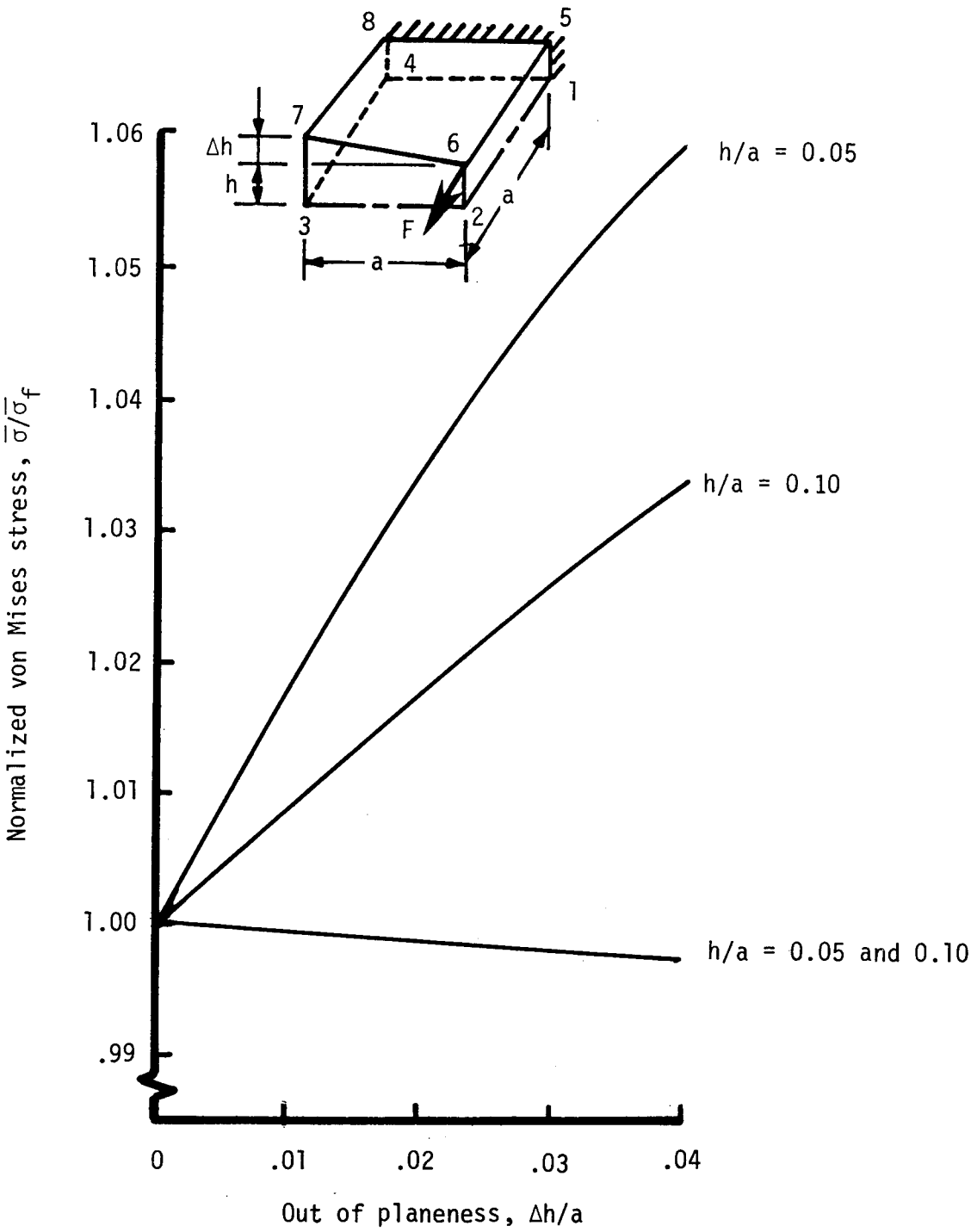

Figure 5.- Scatter of results for centroidal von Mises stress due to out of planeness of node 7 for isotropic material.

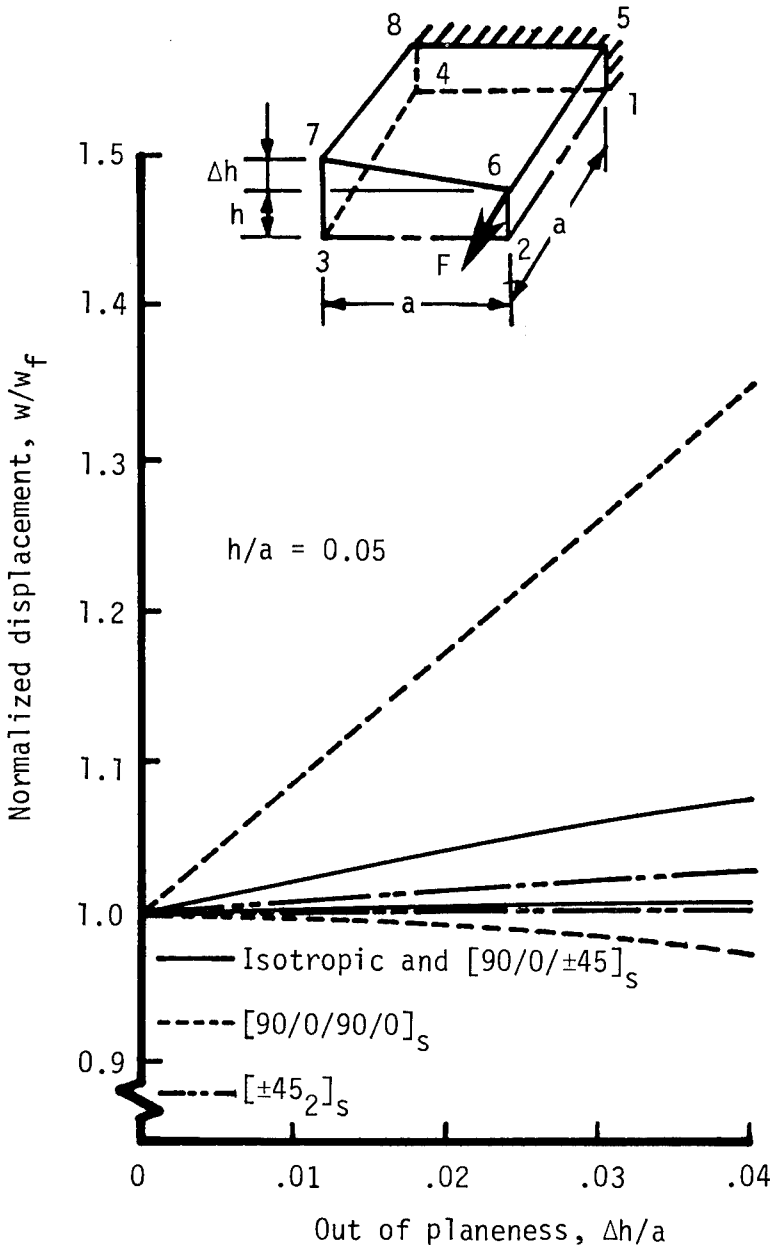

Figure 6.- Effect of out of planeness of node 7 on scatter of normal displacement at node 6 for laminated panel.

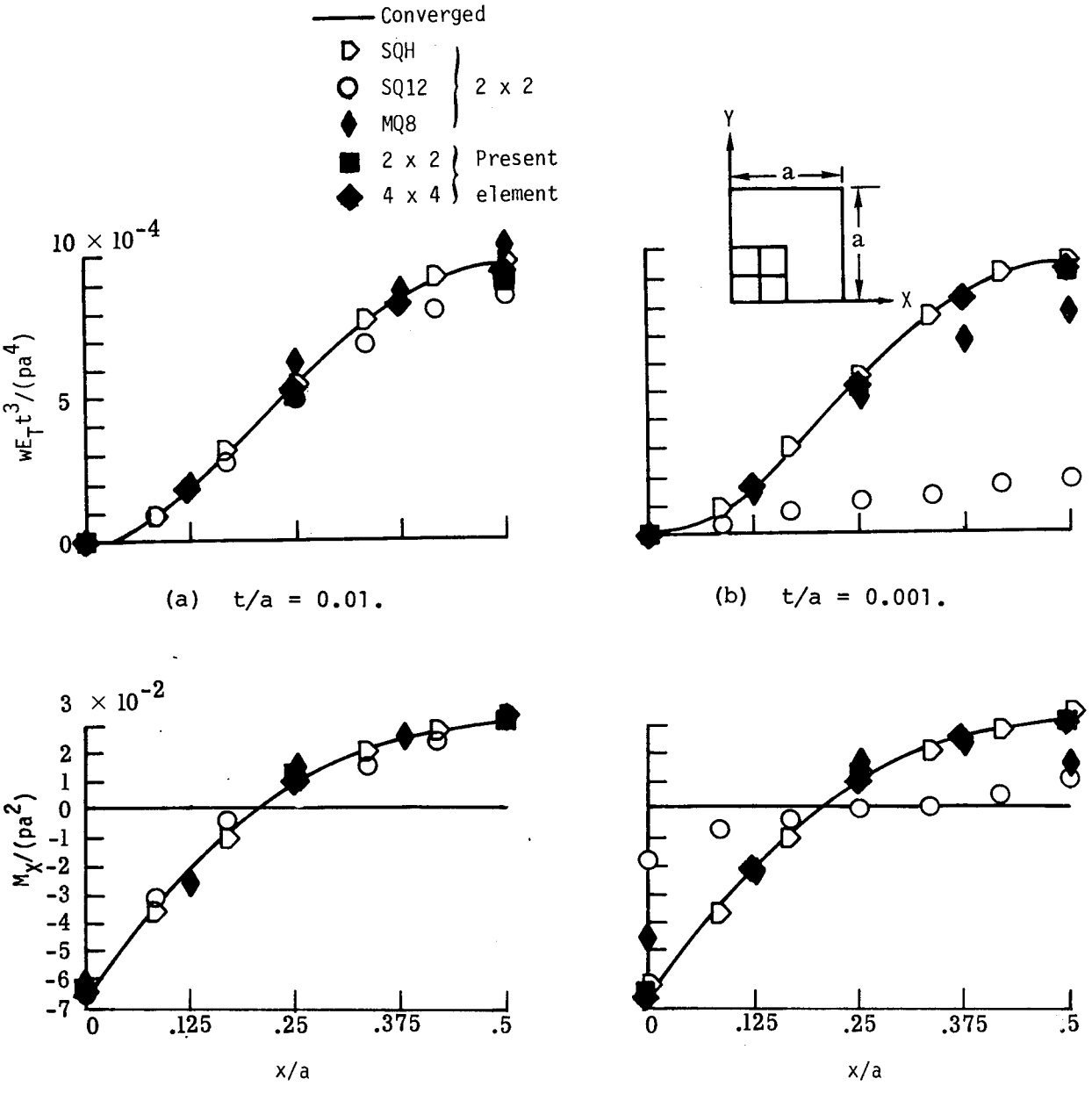

(a) t/a = 0.01.

(b) t/a = 0.001.

(c) t/a = 0.01.

(d) t/a = 0.001.

Figure 7.- Distribution of transverse displacement w and bending-moment resultant M_X along Y = a/2. Clamped, nine-layered [0/90/0/90/0/90/0/90/0], orthotropic square plate (ref. 16).

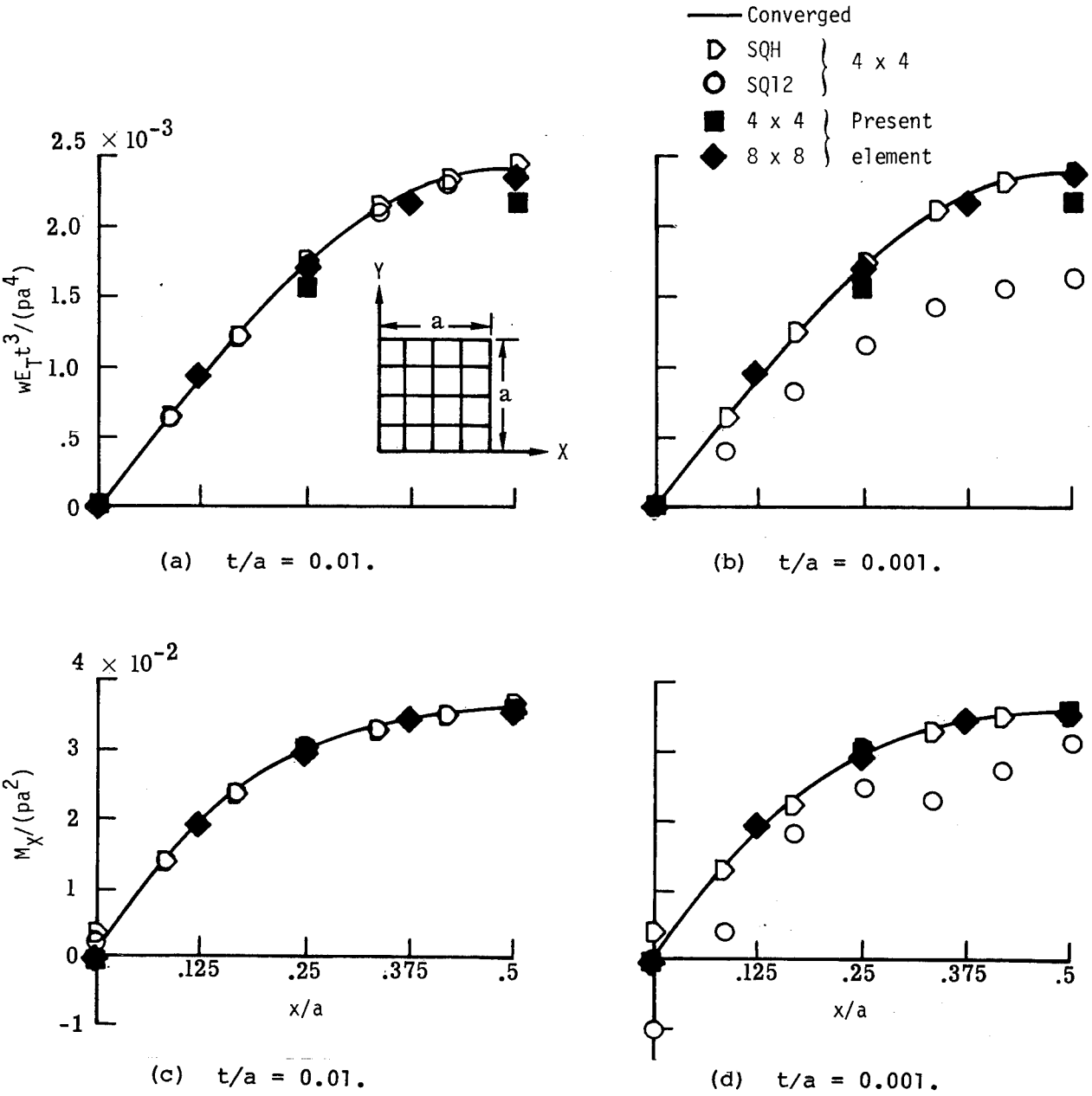

Figure 8.- Distribution of transverse displacement w and bending-moment resultant M_X along Y = a/2. Simply supported, nine-layered [45/-45/45/-45/45/-45/45/-45/45], anisotropic square plate (ref. 16).

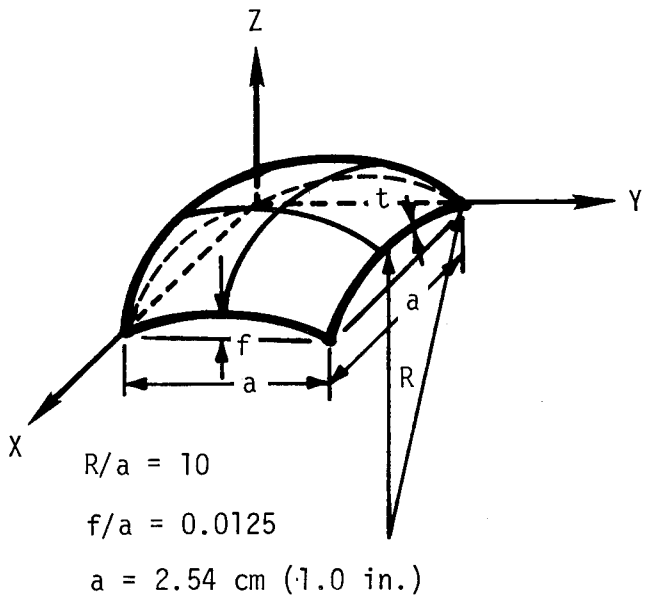

Figure 9.- Geometry of spherical shell model.

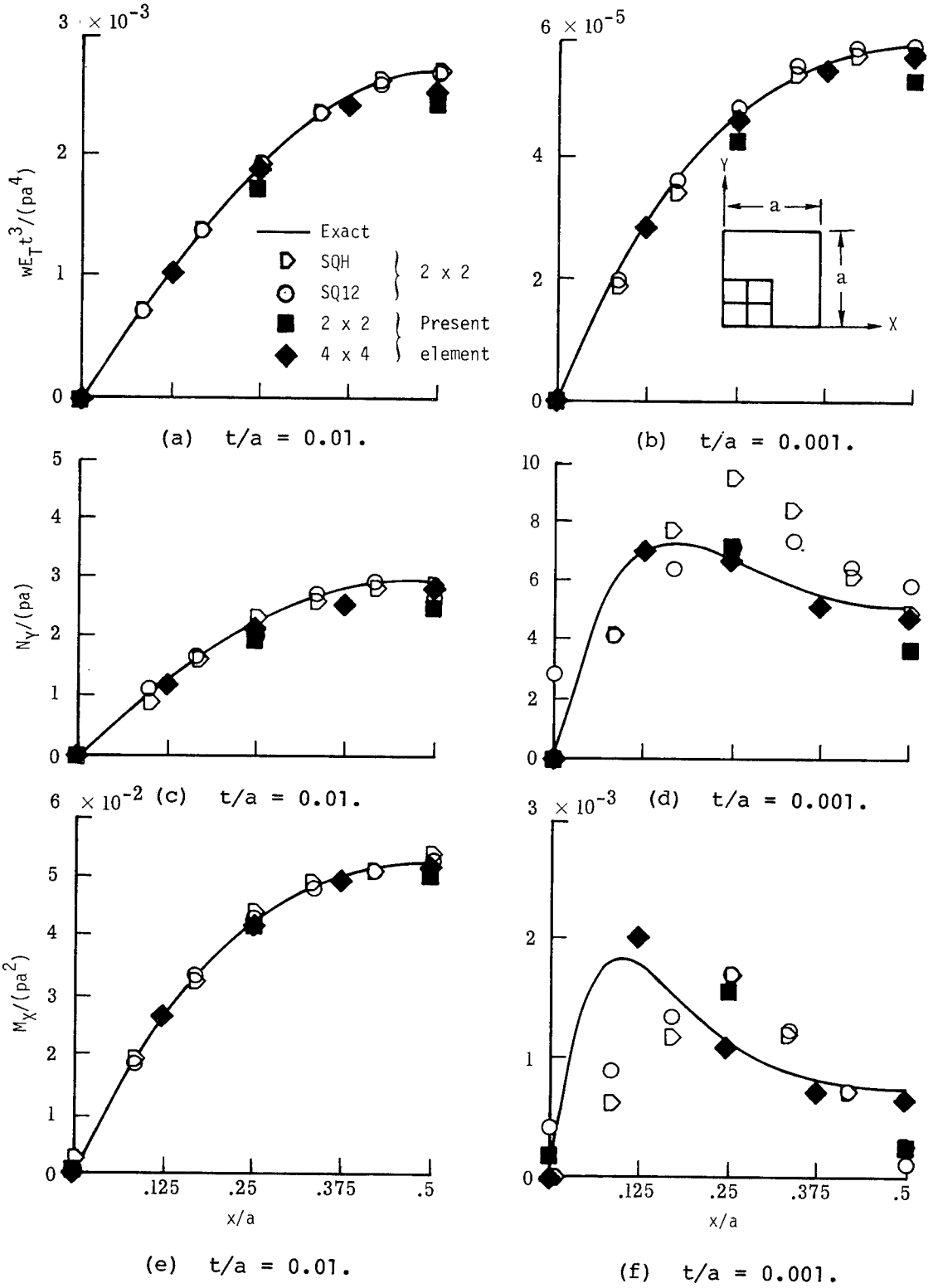

Figure 10.- Distribution of transverse displacement w and stress resultants N_Y and M_X along center lines. Simply supported, nine-layered [0/90/0/90/0/90/0/90/0], orthotropic spherical segments (ref. 16).

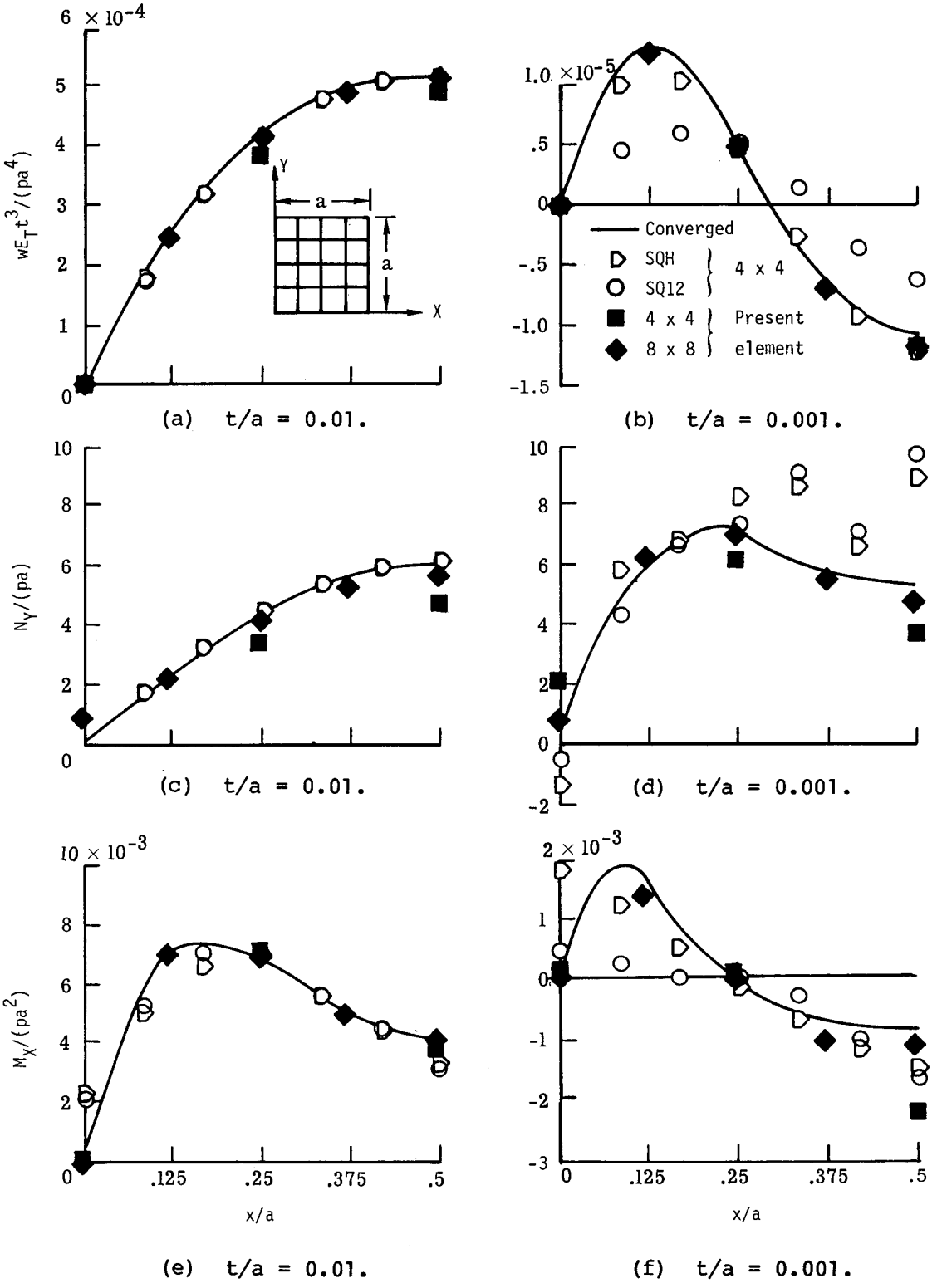

Figure 11.- Distribution of transverse displacement w and stress resultants N_Y and M_X along Y = a/2. Simply supported, nine-layered [45/-45/45/-45/45/-45/45/-45/45], anisotropic spherical segments (ref. 16).

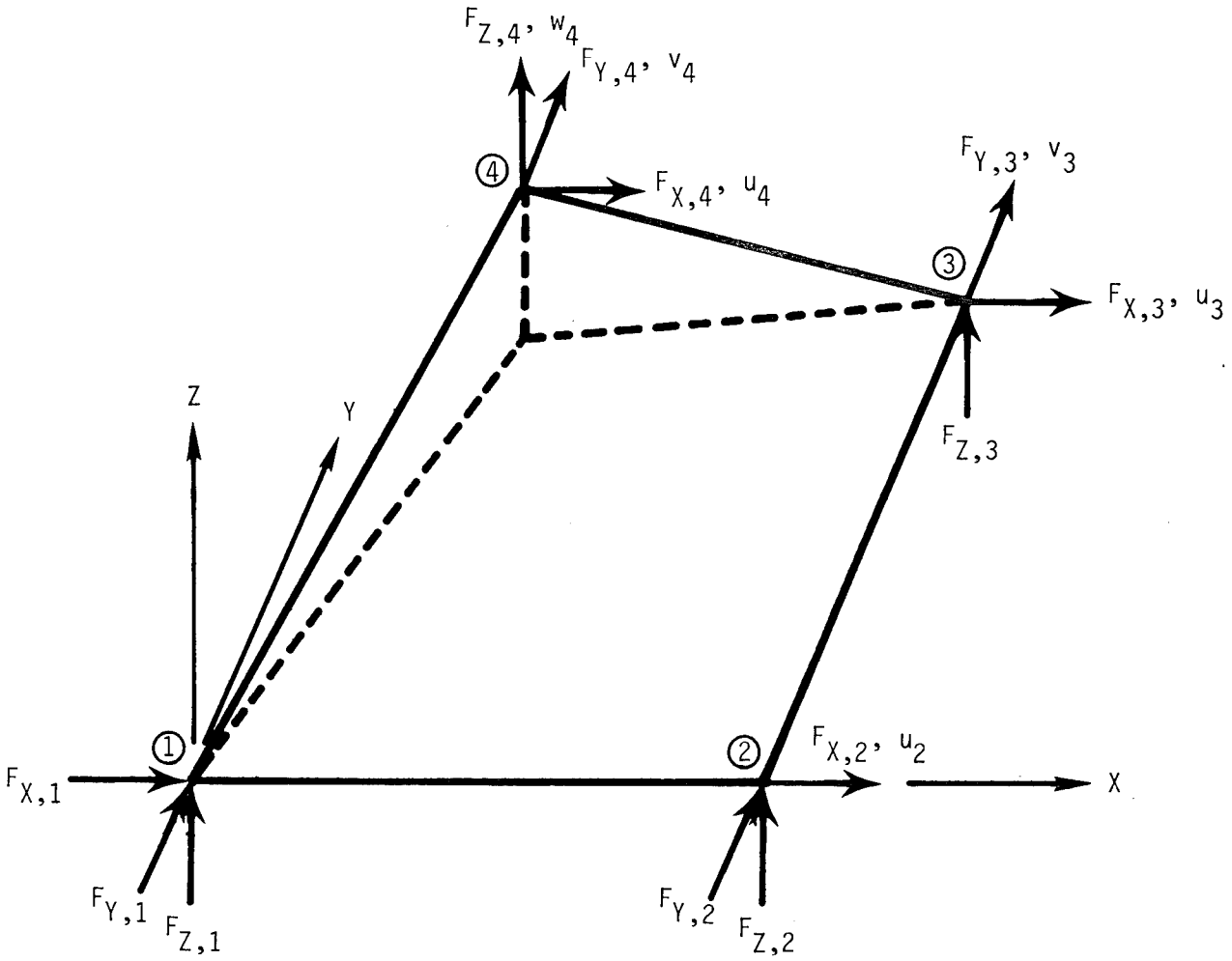

Figure 12.- Forces and displacements on warped membrane element.

1. Report No.	2. Government Accession No.	3. Recipient's Catalog No.
NASA TP-1236		

4. Title and Subtitle	5. Report Date
EVALUATION OF A HYBRID, ANISOTROPIC, MULTILAYERED, QUADRILATERAL FINITE ELEMENT	August 1978
	6. Performing Organization Code
7. Author(s)	8. Performing Organization Report No.
James C. Robinson and Charles L. Blackburn	L-12113
	10. Work Unit No.
9. Performing Organization Name and Address	524-71-03-02
NASA Langley Research Center Hampton VA 23665	11. Contract or Grant No.
	13. Type of Report and Period Covered
12. Sponsoring Agency Name and Address	Technical Paper
National Aeronautics and Space Administration Washington, DC 20546	14. Sponsoring Agency Code

15. Supplementary Notes

James C. Robinson: Langley Research Center.
Charles L. Blackburn: University of Tennessee at Nashville, Nashville, Tennessee.

16. Abstract

A hybrid, anisotropic, multilayered, quadrilateral finite element with bending-extensional coupling is evaluated. Analyses performed in the evaluation include (1) buckling of general laminated plates; (2) thermal stresses of laminated plates cured at elevated temperatures; (3) displacements of a bimetallic beam; and (4) displacement and stresses of a single-cell box beam with warped cover panels. Also, displacements and stresses for flat and spherical orthotropic and anisotropic segments are compared with results from higher order plate and shell finite-element analyses.

17. Key Words (Suggested by Author(s))	18. Distribution Statement
Finite element Laminated composite Warped element Structural analysis	Unclassified - Unlimited Subject Category 39

19. Security Classif. (of this report)	20. Security Classif. (of this page)	21. No. of Pages	22. Price*
Unclassified	Unclassified	28	$4.50

* For sale by the National Technical Information Service, Springfield, Virginia 22161